Mössbauer Studies of $Fe_{1-x}O$. Part I. The Defect Structure of Quenched Samples

By **N. N. Greenwood** *† and **A. T. Howe**, Department of Inorganic Chemistry, The University, Newcastle upon Tyne NE1 7RU

Room-temperature Mössbauer spectra of rapidly quenched samples of nonstoicheiometric $Fe_{1-x}O$ ($0.053 < x < 0.109$) show an envelope of overlapping resonances which, for small values of x, can be resolved into five broad Lorentzian peaks assignable to a series of Fe^{2+} quadrupole doublets and an Fe^{3+} doublet at a lower velocity. As the phase deviates further from stoicheiometry the range of site symmetries produces a more complicated envelope which cannot be resolved into the sum of a small number of Lorentzian peaks. The influence of initial temperature and of quench rate have also been studied over the full range of composition and variations correlated with the known phase diagram for the system. Samples of $Fe_{0.947}O$ which had been most rapidly quenched from 1520 K into water showed negligible disproportionation during quenching. Their spectra, when compared with those predicted for various possible defect structures, suggested the presence of clusters of four vacant cation sites around a tetrahedral Fe^{3+}. Changes in the spectra as the Fe^{3+} content was increased reflected the increase in the defect cluster size towards that previously proposed for $Fe_{0.90}O$ (13 vacant cation sites with 4 tetrahedral Fe^{3+}). Fe^{3+} was present as a quadrupole doublet and no evidence was found for electron hopping between Fe^{2+} and Fe^{3+}. Spectra of the magnetically ordered oxide phases at 77 K were consistent with this interpretation.

SEVERAL conflicting analyses of the room-temperature Mössbauer spectra of quenched samples of $Fe_{1-x}O$ have been reported.[1-5] In view of the current interest in the arrangement of defects in this highly nonstoicheiometric oxide and the applicability of the Mössbauer technique to such systems, a comprehensive Mössbauer investigation of the various forms which exist at different compositions and temperatures has been carried out. In this paper we report an analysis of the room-temperature spectra of samples covering the complete range of composition from $Fe_{0.95}O$ to $Fe_{0.89}O$ and quenched under a variety of conditions. Spectra in the magnetically ordered phases at 77 K were also studied. In Part II the disproportionation reactions which occur in the temperature range 300—700 K are considered and Part III presents the high-temperature Mössbauer spectra obtained on the nonstoicheiometric wüstite phase above 850 K under conditions of equilibrium partial pressure of oxygen.

From the phase diagram in Figure 1 [6,7] it is evident that $Fe_{1-x}O$ is thermodynamically stable only at temperatures above 843 K. Below this temperature disproportionation to the stable products Fe and Fe_3O_4 eventually occurs, though this can be avoided by rapid quenching from the equilibrium state to temperatures at which diffusion is slow.[8] Comparison of the high-temperature X-ray data with data taken on quenched samples [9] shows, however, that a series of metastable phases of $Fe_{1-x}O$ is produced as a result of the rearrangement of defects during the quenching process. Quenched samples of composition $Fe_{0.90}O$ were shown to contain clusters of four tetrahedral Fe^{3+} ions and 13 vacant cation sites arranged so as to give a superlattice three times the basic cubic $Fe_{1-x}O$ unit cell [9] (labelled P′ in Figure 1). The metastable phases P and P′ were found to develop when quenched samples having $x < 0.08$ were heated to temperatures below 623 K.[6] Quenched samples containing higher concentrations of defects

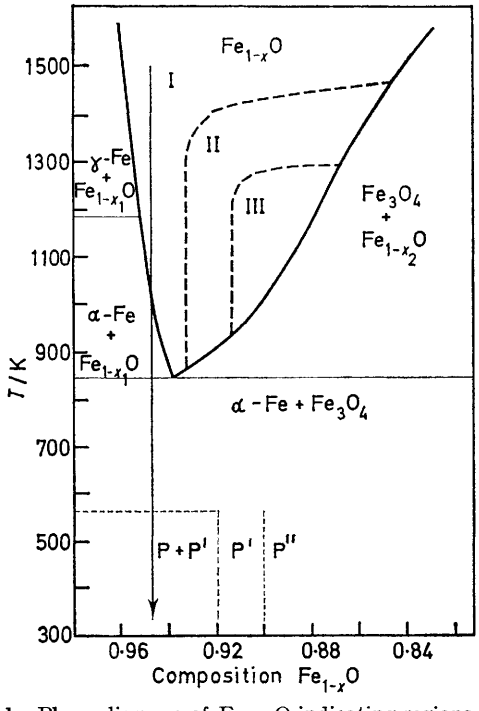

FIGURE 1 Phase diagram of $Fe_{1-x}O$ indicating regions through which samples pass during quenching to room temperature (see arrow). Dotted lines demark the low-temperature metastable phases P, P′ and P″ and the heavier dashed lines demark the regions I, II, and III in the stable high-temperature wüstite phase field

($x > 0.10$) showed nuclei of Fe_3O_4 together with an ordered phase P″ having a superlattice five times larger

† *Present address:* Department of Inorganic and Structural Chemistry, The University of Leeds, Leeds LS2 9JT

[1] G. K. Wertheim, *J. Applied Phys.*, 1961, **32**, 110S.
[2] G. Shirane, D. E. Cox, and S. L. Ruby, *Phys. Rev.*, 1962, **125**, 1158.
[3] D. J. Elias and J. W. Linnett, *Trans. Faraday Soc.*, 1969, **65**, 2673.
[4] D. P. Johnson, *Solid State Comms.*, 1969, **7**, 1785.
[5] H. Schechter, P. Hillman, and M. Ron, *J. Appl. Phys.*, 1966, **37**, 3043.
[6] J. Manenc, *Bull. Soc. Franc. Mineral Cryst.*, 1968, **91**, 594.
[7] B. E. F. Fender and F. D. Riley, *J. Phys. Chem. Solids*, 1969, **30**, 793.
[8] C. Carel, *Mem. Sci. Rev. Met.*, 1967, **64**, 821.
[9] F. Koch and J. B. Cohen, *Acta Cryst.*, 1969, *B***25**, 275.

than that of the basic unit cell.[6] The regions of occurrence of the metastable phases are shown in Figure 1.

It would be expected that the Mössbauer parameters, which are sensitive to local defect arrangements [10] would reflect such transformations at an earlier stage of defect aggregation than could be detected by *X*-ray spectroscopy or electron microscopy, and the Mössbauer spectra of quenched samples should thus be very dependent on the quenching conditions. Since these considerations have not been previously investigated, we have studied the Mössbauer spectra as a function of quenching rate over a wide range of composition in order to determine the possible influence of such transformations, and to investigate the defect structure of the metastable phases. Accurate analysis of the spectra was made possible by the use of thin absorbers in order to reduce saturation effects.[11]

EXPERIMENTAL

Samples were prepared by equilibrating 50—100 mg Fe_2O_3 (<50 p.p.m. impurities) in a CO_2–CO gas stream at 1520 K for 2 h, sometimes followed by annealing for longer periods at lower temperatures. After the initial sintering had occurred (several minutes) the samples were withdrawn from the furnace and reground to provide the maximum surface area for subsequent rapid cooling. Quenching was achieved within the controlled atmosphere by dropping the shallow platinum bucket containing the sample directly into chilled water or mercury, as described by Carel.[8] The composition of the samples, as set by the CO_2–CO ratio [12,13] to a relative accuracy of $\pm 0{\cdot}002$ in x, was checked against the observed lattice parameters, and agreed with the data of Carel.[8] The *X*-ray photographs showed no evidence of reaction products of $Fe_{1-x}O$ with either water or mercury.

The powders were ground under acetone, mixed with Apiezon grease, and loaded into the Mössbauer holders to a density of 10 mg cm^{-2} for the room temperature spectra, and 20—30 mg cm^{-2} for the magnetically split spectra. Care was taken to ensure uniform sample distribution by grinding the powders in an agate mortar until individual particles could not be seen when viewed against the light after grease had been added and the sample had been spread into the holder. Resonant absorptions for the two types of spectra (measured as a decrease in count rate) ranged between 10—15 and 3—6% respectively. The spectrometers used were of standard design,[14] and were arranged so that geometrical effects would be insignificant even for the high-quality spectra. Some spectra were also obtained from the P.C.M.U., Harwell. Chemical isomer shifts are expressed relative to the centroid of the spectrum of iron metal at 295 K.

RESULTS AND DISCUSSION

(a) *The Influence of Quench Rate on the Mössbauer Spectra.*—The effectiveness of various quenching methods was gauged by the extent to which samples having a high concentration of defects ($x > 0{\cdot}10$) disproportionated to Fe_3O_4 during the cooling process. A water quench was found to be more rapid than a quench into mercury. Quenching in the gas stream alone produced large quantities of Fe_3O_4 and was therefore not used. For compositions with $x < 0{\cdot}10$ no appreciable transformation to Fe_3O_4 occurred for either water- or mercury-quenched samples, but the spectra of $Fe_{1-x}O$ were different for the two methods and a comparison of the spectra obtained enabled the effect of the quench rate to be investigated.

The effect of the slower quench into mercury depended on the composition of the sample and the temperature from which it was quenched. Three types of behaviour were found, as illustrated by the spectra shown in Figure 2 for three appropriate compositions, and were as follows. (i) For samples of composition $Fe_{0{\cdot}947}O$ the spectra showed a marked dependence on both quench rate and initial temperature. Neither Fe nor Fe_3O_4 was detected in the high-velocity Mössbauer spectra of samples quenched from 1520 and 1200 K (detection limit 0·5%), showing that the observed transformations preceded the composition to Fe_3O_4. Peaks of Fe_3O_4 were just discernible at low velocity in the spectrum of $Fe_{0{\cdot}947}O$ quenched from 1050 K into mercury.

(ii) For samples of composition $Fe_{0{\cdot}900}O$ there was very little dependence on either the quench rate or the equilibration temperature, as shown in Figure 2. Neither Fe nor Fe_3O_4 was detected in the high-velocity spectra.

(iii) For more grossly nonstoicheiometric wüstite, as shown for $Fe_{0{\cdot}891}O$ in Figure 2, there was again a pronounced dependence on both the quench rate and equilibration temperature. Only at the highest temperature and fastest quench rate could samples be obtained free from Fe_3O_4 peaks in the spectra. Samples quenched into mercury showed extensive disproportionation to Fe_3O_4. There was no evidence in any of the samples for the presence of superparamagnetic domains of Fe_3O_4 since the spectra behaved normally over a wide range of temperatures down to 77 K and the spectral features were invariant with increasing particle size.

More extensive work established that the composition ranges within which these three types of behaviour occurred coincided with the three regions of the metastable phases found by Manenc [6] (see Figure 1). For samples having small values of x, Manenc observed a disproportionation to the P and P′ phases after short periods of reheating at temperatures below 623 K. The observed diminution of the quadrupole splitting of the less rapidly quenched samples of $Fe_{0{\cdot}947}O$ can be identified with such a disproportionation actually occurring during the quenching process, although the extent of the reaction was not sufficient to cause any change in the *X*-ray powder pattern. By contrast, Manenc found no such disproportionation in the region of $Fe_{0{\cdot}900}O$ (P′

[10] N. N. Greenwood, A. T. Howe, and F. Ménil, *J. Chem. Soc.* (*A*), 1971, 2218.
[11] T. C. Gibb, R. Greatrex, and N. N. Greenwood, *J. Chem. Soc.* (*A*), 1968, 890.
[12] L. S. Darken and R. W. Gurry, *J. Amer. Chem. Soc.*, **1945**, **67**, 1398.
[13] R. J. Ackermann and R. W. Sandford, jun., U.S. Atomic Energy Commission Research and Development Report, 1966, ANL-7250.
[14] N. N. Greenwood and A. T. Howe, Proc. Apollo 11 Lunar Science Conf. vol. 3, *Geochim. Cosmochim. Acta, Suppl. I*, 1970, 2163.

phase), and the lack of dependence of the Mössbauer spectra on the quench rate for this composition is consistent with this. The rapid precipitation of Fe_3O_4 from samples of $Fe_{0.891}O$ agrees with the behaviour of the P″ phase found by Manenc. There was no evidence from the spectra of defect aggregation during cooling through the high-temperature regions, and the slightly differing defect structures anticipated at the various high temperatures [7,15] appear to be frozen in and to act as nuclei for the low-temperature transformations which therefore proceeded at different rates. The effect was manifest as a dependence of the spectra on the temperature from which the samples were quenched, particularly in the limiting cases of $Fe_{0.947}O$ and $Fe_{0.891}O$.

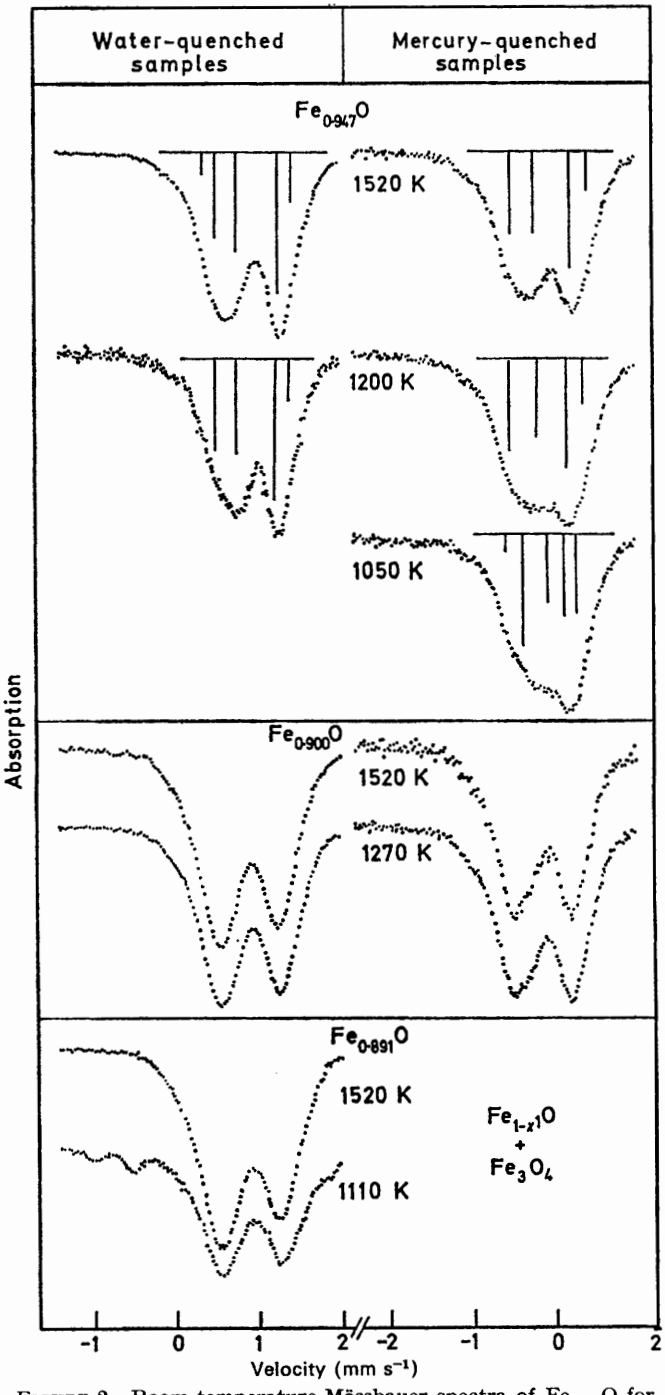

FIGURE 2 Room-temperature Mössbauer spectra of $Fe_{1-x}O$ for three typical compositions; the samples were quenched into water or mercury from the temperatures indicated

The intensities and velocities of the computer-resolved peaks of the spectra of $Fe_{0.947}O$ are represented in Figure 2 by the vertical lines. The four major peaks do not behave as two resolvable quadrupole doublets, as can be seen from their varying intensities (and also varying areas). In sections (b) and (d) it will be shown that this behaviour arises because there are a large number of quadrupole-split resonances of slightly differing parameters which overlap to produce the total envelope to which the best resolvable approximation is a four- or five-peak fit. The observed changes in the spectra can, however, be gauged by assuming that the predominant components of the envelope occur at the velocities indicated by the lines in Figure 2. A discussion in these terms is given below, where the parameters refer to the two outer velocities as representing one quadrupole doublet, and to the two inner velocities as representing the other doublet, an assignment which results in the two doublets having similar values of the isomer shift.

For $Fe_{0.947}O$ quenched into water from 1520 K the quadrupole splittings, Δ, are 0·92 and 0·51 mm s^{-1} and the chemical isomer shifts, δ, are 0·97 and 1·00 mm s^{-1} respectively. The decreased resolution found for the spectrum of the corresponding sample quenched into mercury from 1520 K is due to a reduction in the quadrupole splitting of the inner components. The parameters of the two doublets in this case are $\Delta = 0{\cdot}93$ and 0·44 mm s^{-1} and $\delta = 0{\cdot}91$ and 0·95 mm s^{-1} respectively.

More marked changes were evident in the spectrum of $Fe_{0.947}O$ quenched into mercury from the lowest temperatures, *e.g.* the sample quenched from 1050 K showed traces of Fe_3O_4 together with a significant reduction in the quadrupole splitting of both doublets, the parameters of which were $\Delta = 0{\cdot}65$ and 0·21 mm s^{-1} and $\delta = 0{\cdot}95$ and 1·02 mm s^{-1} respectively.

(b) *Spectral Analysis of Rapidly Quenched Samples.*— Spectra of water-quenched samples covering almost the complete composition range possible at 1520 K are shown in Figure 3. Samples quenched under these conditions showed the least evidence of transformation during cooling. In computing these spectra, 10 different model assignments were assessed for goodness of fit. For $Fe_{0.947}O$ an acceptable fit was obtained with five peaks (shown in Figure 3); the value [16] of χ^2 was 526 for 164 degrees of freedom. The minimum values of χ^2 for assignments using 2, 3, 4, and 6 peaks were 2351, 884, 858, and 3200 respectively. Attempts at constraining some or all of the parameters of possible quadrupole

[15] P. Raccah and P. Vallet, *Mem. Sci. Rev. Met.*, 1965, **62**, 1.
[16] B. J. Duke and T. C. Gibb, *J. Chem. Soc.* (*A*), 1967, 1478.

doublet peaks to be equal in intensity invariably resulted in fits with higher values of χ^2.

Such an acceptable solution could not be found for the spectrum of $Fe_{0.900}O$. Fits with 2, 3, 4, 5, and 6 peaks (173—161 degrees of freedom) gave minimum values of χ^2 of 1461, 1360, 1608, 3700, and 3750 respectively. In this case it is clear that many more component peaks overlap to produce a complicated envelope which cannot be resolved into the sum of a small number of Lorentzian peaks. Indeed, it was found, in general, that only for small values of x could a detailed interpretation in terms of the resolvable component peaks be made: as the Fe^{3+} content increases the analysis becomes indeterminate. This could well account for the lack of agreement in the various analyses so far reported.[1-5]

In a recently published detailed analysis [4] Johnson fitted the spectra of samples ranging from $Fe_{0.935}O$ to $Fe_{0.905}O$ with 5 peaks, but constrained the parameters to represent two quadrupole doublets, assigned to Fe^{2+}, whilst a low-velocity peak was assigned to Fe^{3+}. Changes in the ratio of the intensities of the two Fe^{2+} doublets with composition were then interpreted in terms of the p–n transition observed at high temperature.

The present analysis of $Fe_{0.947}O$, using unconstrained parameters shows that the low-velocity peak at 0·28 mm s^{-1} (labelled A in Figure 3), accounts for only 6·5% of the total resonance area, compared to the calculated proportion of 11·2% of Fe^{3+} in the sample. The low chemical-isomer shift and low intensity suggest that peak A is but one component of a quadrupole-split Fe^{3+} doublet: peaks at positions A and C would give a chemical isomer shift (0·48 mm s^{-1}) typical of Fe^{3+} in octahedral oxygen co-ordination with a small quadrupole splitting (0·40 mm s^{-1}) arising from neighbouring defects. Similar parameters have been reported for the cluster of two Fe^{3+} cations adjacent to a cation vacancy in doped MgO lattices.[17] This assignment also has the attraction that the Fe^{2+} component of peaks B and C would then have more nearly the same area as the combined area of peaks D and E. On this basis *ca.* 13% of the total resonance area arises from Fe^{3+} and *ca.* 87% from Fe^{2+}, compared with the proportions of 11·2 and 88·8% calculated from the known composition of the sample. This agreement is satisfactory considering the assumptions made. Furthermore, any correction due to saturation effects [11] would result in the *relative* area of the small peak A being reduced slightly, thus tending to improve the agreement still further. This can be seen since the reduction in absorption caused by saturation is greater for regions at which the absorption is larger, thus the area of the Fe^{2+} resonance would be increased more by the correction than that of Fe^{3+}.

Further refinements to the computer analysis, namely the introduction of the high-velocity component of the proposed Fe^{3+} doublet to match peak A, and the introduction of a small quadrupole doublet (δ *ca.* 0·25 mm s^{-1}, Δ ranging from 0 to 0·4 mm s^{-1}) to represent any Fe^{3+} on tetrahedral sites did not yield lower sums of residuals. In the present case, however, this does not refute the presence of such peaks, but simply reflects the fact that

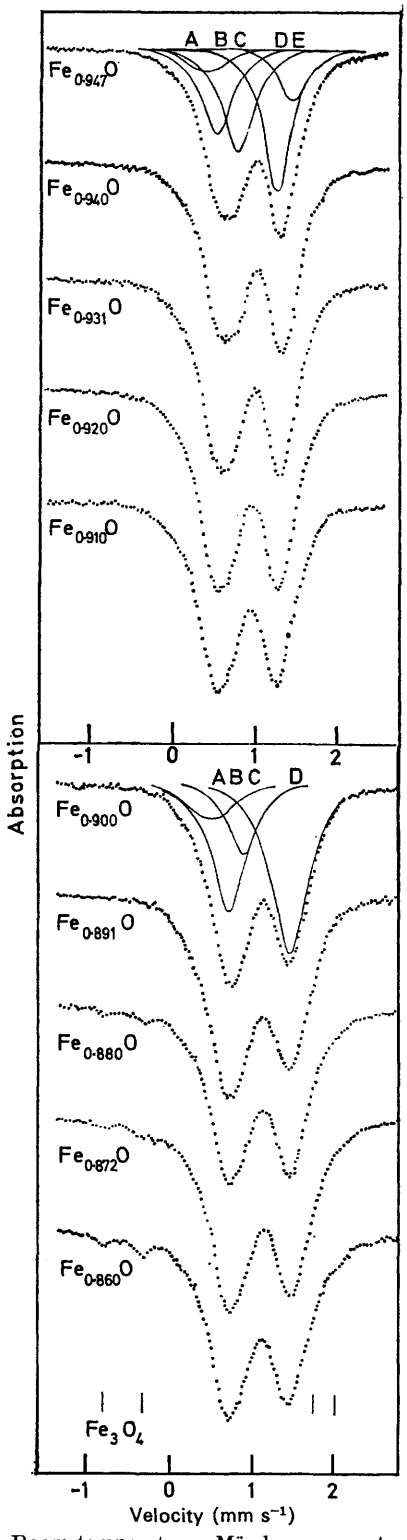

FIGURE 3 Room-temperature Mössbauer spectra of $Fe_{1-x}O$ quenched from 1520 K into water, showing the progressive change of the resonance profile as a function of composition. For interpretation of peaks A—E see text

[17] U. Gonser, R. W. Grant, H. Wiedersich, R. Chang, and A. H. Muir, *Bull. Amer. Phys. Soc.*, 1965, **10**, 709.

the resolution of the minor peaks is limited by the approximate nature of the fit to the major components.

No evidence was found for electron hopping between Fe^{2+} and Fe^{3+} at a rate commensurate with the ^{57}Fe excited state lifetime (*ca.* 100 ns). Spectra were simulated for three models assuming that the number of Fe^{2+} cations involved in the exchange process was equal to (*a*) the number of Fe^{3+} cations present, (*b*) twice the number of Fe^{3+} cations, and (*c*) the sum total of all the Fe^{2+} ions present. In none of these cases could the observed spectra be generated. The earlier interpretation [3] of a 3-peak fit to the spectra of oxides in the range $Fe_{0.94}O$ to $Fe_{0.92}O$ in terms of exchange between Fe^{2+} and Fe^{3+} ions is, therefore, not consistent with the present more extended set of data. A conduction mechanism consistent with both the Mössbauer results and the observed high electronic conductivity [18] would be an electron hopping which, because it occurred between sites of slightly different defect environment, was slower than the hopping which is known to average the Mössbauer spectra of Fe^{2+} and Fe^{3+} ions on the equivalent octahedral sites of Fe_3O_4 at room temperature.[19,20]

As the Fe^{3+} content of the samples increases from 11·2% in $Fe_{0.947}O$ to 22·2% in $Fe_{0.900}O$ the relative intensity of the low-velocity peaks A and B increases and the quadrupole splitting of the Fe^{2+} component increases so that part of the C resonance in $Fe_{0.947}O$ appears with peak B in $Fe_{0.900}O$. At still higher Fe^{3+} concentration peaks from Fe_3O_4 are increasingly evident and the spectra of the residual $Fe_{1-x}O$ are similar to that of $Fe_{0.910}O$.

(c) *Magnetic Spectra at* 77 K.—Below the Néel temperature of $Fe_{1-x}O$ of *ca.* 200 K (ref. 21) a magnetocrystalline distortion to a rhombohedral structure occurs.[22] Spectra obtained at 77 K for this structure are shown in Figure 4, for some of the typical compositions already discussed. The spectrum can be resolved into an Fe^{3+} pattern ($H_{eff} = 480 \pm 10$ kG) and an Fe^{2+} pattern ($H_{eff} = 340 \pm 20$ kG). The resonance linewidths are very broad at the extreme velocities, particularly for the case of Fe^{2+}, a feature which is characteristic of a range of magnetic and possibly quadrupole interactions.[10]

The Fe^{3+} pattern, which becomes more intense for larger values of x as expected, shows no evidence of electron hopping with Fe^{2+}, nor any indication of superparamagnetic behaviour. It is also sufficiently different from the known spectrum of Fe_3O_4 in overall appearance and detailed parameters [19,20] to indicate that the Fe^{3+} ions in quenched samples of $Fe_{1-x}O$ are not present as microdomains of Fe_3O_4.

The Fe^{2+} magnetic spectrum of $Fe_{.0947}O$ was sharper for the sample quenched from 1050 K into mercury than for that quenched into water from 1520 K, which is consistent with a less random defect distribution in the mercury-quenched sample. It is also clear from Figure 4 that an increase in the defect concentration as the composition deviates further from stoicheiometry broadens the Fe^{2+} resonance, as shown for $Fe_{0.900}O$ and $Fe_{0.891}O$. No significant difference was evident in the magnetic spectra of these two phases, P′ and P″.

(d) *Structural Model for the Defects in* $Fe_{1-x}O$.—It will be convenient to consider first the defect structure in samples rapidly quenched from 1520 K into water and then to discuss those samples which showed evidence for more extensive transformation during quenching.

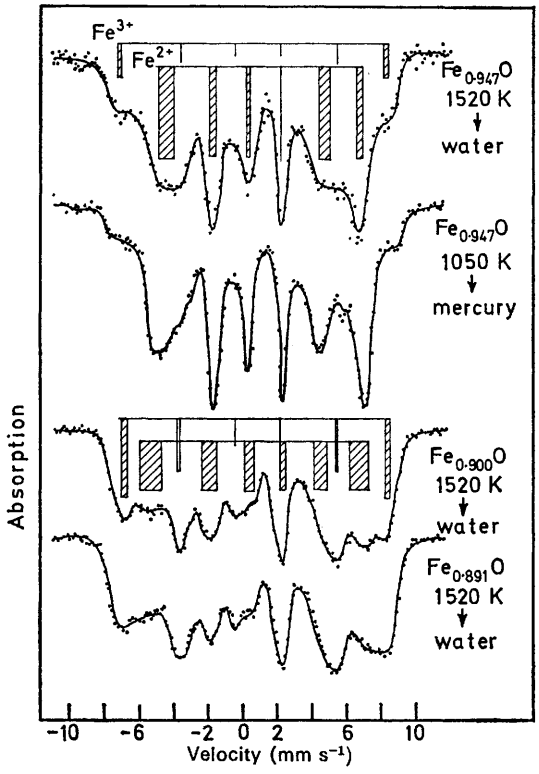

FIGURE 4 Mössbauer spectra of $Fe_{1-x}O$ at 77 K. The temperature from which the samples were quenched and the quenching liquid are indicated in the right-hand margin. Approximate assignments of the broad peaks are shown in the bar diagrams

The room-temperature spectra of samples quenched from 1520 K into water can be related to the defect structure through the quadrupole splitting of Fe^{2+}. When Fe^{2+} is doped at very low concentration into the cubic lattice of MgO a single resonance with zero quadrupole splitting is observed at room temperature.[23] However, in the presence of an adjacent cation vacancy, such as occurs for Fe^{2+} doped into the cubic lattice of NaCl, a quadrupole splitting of *ca.* 0·5 mm s^{-1} was found.[24] This arises from the electric-field gradient produced at the nucleus by the unequal electron population of the now non-degenerate T_{2g} levels. In the case of $Fe_{1-x}O$, further distortions from cubic symmetry caused by

[18] I. Bransky and D. S. Tannhauser, *Physica*, 1967, **37**, 547.
[19] W. Kündig and R. S. Hargrove, *Solid State Comms.*, 1969, **7**, 223.
[20] G. A. Sawatzky, J. M. D. Coey, and A. H. Morrish, *J. Applied Phys.*, 1969, **40**, 1402.
[21] F. B. Koch and M. E. Fine, *J. Appl. Phys.*, 1967, **38**, 1470.
[22] B. T. M. Willis and H. P. Rooksby, *Acta Cryst.*, 1953, **6**, 827.
[23] H. R. Leider and D. N. Pipkorn, *Phys. Rev.*, 1968, **165**, 494.
[24] J. G. Mullen, *Phys. Rev.*, 1963, **131**, 1415.

more than one adjacent vacancy or by adjacent Fe^{3+} cations would be expected to further split the T_{2g} levels and cause a larger quadrupole splitting. This valence contribution to the electric-field gradient is expected to be much larger than that from the lattice charges, which may depend on the relative orientation of the surrounding defects.

We have based the present calculations on the cluster structures recently established by diffraction experiments. The smallest cluster was taken to be 4 vacant cation sites situated around one tetrahedral Fe^{3+}, represented as $\{^{t}Fe^{3+}(\square_{+})_4\}^{5-}$; this was the minimum cluster size indicated by neutron diffraction measurements in the high temperature region.[25] The largest cluster was taken to be $\{^{t}Fe^{3+}{}_4(\square_{+})_{13}\}^{14-}$, as found for the P′ phase discussed earlier.[9]

The two clusters are shown diagrammatically in Figure 5. The proportion of Fe^{2+} ions which have 0—9 defects (taken as Fe^{3+} or vacant cation sites) at any of the 18 surrounding cation positions in the lattice is shown in Figure 5, for the two cluster sizes for the compositions $Fe_{0.918}O$ and $Fe_{0.947}O$. The cation positions which most influence the quadrupole splitting have been taken as the 12 nearest-neighbour cation sites plus the six next-nearest-neighbour cation sites on the far side of the six oxygen ions which octahedrally coordinate the Fe^{2+}. It has been assumed that the clusters are evenly distributed throughout the lattice and that the Fe^{3+} ions which are not on tetrahedral sites only occupy those sites which have a lower electrostatic potential due to the presence of vacancies at any of the 18 neighbouring positions. Such an Fe^{3+} distribution, which enables the charge carriers to move preferentially along paths of low-potential cation sites is suggested by conductivity studies.[18] For the single cluster there are 36 such sites peripheral to the cluster of four vacancies. These are filled by 5 Fe^{3+} (thus balancing the five-fold negative charge on the cluster) and 31 Fe^{2+}. Each of the 31 peripheral Fe^{2+} has either 1 or 3 neighbouring vacant sites and 4, 7, or 9 neighbouring peripheral sites, the occupancy of which was calculated as the probability of 0, 1, . . . 9 Fe^{3+} ions, where 5/36 was the probability that any one of the sites would be occupied by Fe^{3+}. The remaining non-peripheral Fe^{2+} (approximately 16 per cluster in the case of $Fe_{0.947}O$) have only neighbouring Fe^{3+} ions, the number of which was again calculated from the above probability. The histograms shown in Figure 5 were obtained after summing over all Fe^{2+} ions in the lattice. For the four-fold cluster, 14 Fe^{3+} and 40 Fe^{2+} were randomised over the 54 peripheral sites around each cluster, and the results are also shown in Figure 5.

It can be seen that the two histograms for $Fe_{0.947}O$ predict quite different combinations of quadrupole splittings of Fe^{2+}. The two major quadrupole doublets of the observed spectra (see Figure 3) are well accounted for by the single-cluster model for which a high proportion of Fe^{2+} cations have one and two neighbouring defects, with the other configurations merely contributing to the spread of the peaks. The spectrum is, therefore, consistent with the presence of single clusters in $Fe_{0.947}O$ which has been quenched into water from 1520 K.

In the case of $Fe_{0.918}O$ the two histograms do not predict significantly different quadrupole splitting distributions. However, at this composition, which was chosen for the calculations because it corresponds to the perfectly ordered three-fold superlattice,[9] the four-fold clusters occur, as previously discussed, and the Mössbauer

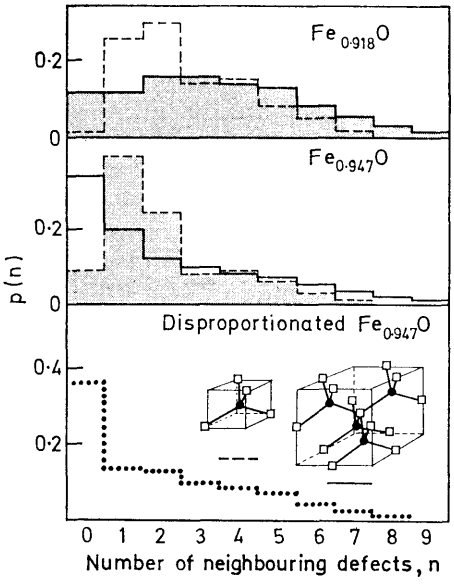

FIGURE 5 Histograms showing the proportion, p(n), of Fe^{2+} ions having 0—n neighbouring defects (Fe^{3+} or cation vacancies) calculated for the single-cluster model (dashed line) and the four-fold-cluster model (full line) for two typical compositions. The effect of disproportionation on defect distribution is shown by the bottom line in the bottom histogram (see text)

spectra of samples of similar composition are consistent with this.

The relevant distributions have been shaded in Figure 5. The change from single clusters in $Fe_{0.947}O$ to four-fold clusters in $Fe_{0.918}O$ results in an increase in the number of Fe^{2+} ions having more than two neighbouring defects, and this is reflected in the Mössbauer spectra as a reduction in the intensity of peak C whilst that of peak B increases. The wide range of Fe^{2+} environments and the consequent large range of quadrupole splittings explains the inadequacy of the attempted computer fits to the spectra of $Fe_{0.900}O$.

We turn finally to a consideration of samples showing extensive transformation during quenching. The presence of Fe_3O_4 in the sample of $Fe_{0.947}O$ quenched from 1050 K into mercury shows that the decomposition was in an advanced stage and the products could be compared with those found by Manenc in quenched samples of $Fe_{0.95}O$ which had been reheated for short periods of time. For example, after 5 min at 573 K the X-ray

[25] A. K. Cheetham, B. E. F. Fender, and R. I. Taylor, *Solid State Phys.*, 1971, **4**, 2160.

pattern showed satellite lines and electron microscopy showed intergrown lamellae 100—500 Å thick of defect-rich (P′) and defect poor (P) phases.[26,27] Such a decomposition of $Fe_{0.947}O$, represented as

$$2Fe_{1-x}O \longrightarrow Fe_{1-x-y}O + Fe_{1-x+y}O$$

would finally produce the P′ phase, taken to be the composition of the perfectly ordered structure, $Fe_{0.918}O$,[9] together with $Fe_{0.976}O$. The distribution of defects around the Fe^{2+} ions in such a mixture, assuming four-fold clusters in $Fe_{0.918}O$ and single clusters in $Fe_{0.976}O$, is shown in Figure 5. The large proportion of Fe^{2+} ions having no neighbouring defects is consistent with the small quadrupole splitting of the resolved inner doublet shown in Figure 2, while the outer doublet represents Fe^{2+} ions with one or more neighbouring defects.

The intermediate range of quadrupole splittings present in samples of $Fe_{0.947}O$ quenched into mercury from 1520 and 1200 K is consistent with partial defect segregation. The possibility of detecting an initial growth in cluster size preceding the long-range variations in composition can be examined by comparing the neighbouring defect distributions for the case of single and four-fold clusters in $Fe_{0.947}O$. Figure 5 shows that the Mössbauer spectra would be sensitive to such a growth in cluster size, as represented by the equation

$$4\{^{t}Fe^{3+}(\square_{+})_{4}\}^{5-} \longrightarrow \{^{t}Fe^{3+}{}_{4}(_{+}\square)_{13}\}^{14-} + 3\square_{+}.$$

However, the histogram for the four-fold cluster is not sufficiently different from that of the extensively decomposed $Fe_{0.947}O$ to enable a confirmation of such a primary step by this technique alone. Recent *X*-ray evidence suggests spinodal decomposition in quenched samples of $MgO–Fe_{1-x}O$ solid solutions;[28] a similar situation might be expected in $Fe_{1-x}O$ and could be described by the above defect aggregation. However, the process is complicated by the growth of the P′ phase, which may occur *via* nucleation rather than as an end product of spinodal decomposition.

We thank the Association of Commonwealth Universities for a scholarship (to A. T. H.), the S.R.C. for financial support, and Dr. B. E. F. Fender for communication of results prior to publication.

[1/924 *Received, June 7th,* 1971]

[26] J. Manenc, *J. Phys.*, 1963, **24**, 447.
[27] T. Herai, B. Thomas, J. Manenc, and J. Bénard, *Compt. rend.*, 1964, **258**, 4528.
[28] S. K. Evans and I. B. Cutler, *J. Material Sci.*, 1970, **5**, 141.